# Combining Wavelet Transform and Graph Theory for Feature Extraction and Visualization

*Christoph Lürig* *Roberto Grosso* *Thomas Ertl*

Lehrstuhl für Graphische Datenverarbeitung (IMMD 9)
Universität Erlangen-Nürnberg
Am Weichselgarten 9, 91058 Erlangen

**Abstract.** In the process of visualizing 3D MRI or CT data using techniques such as isosurfacing or direct volume rendering, one is confronted with two problems. The first one is that there is no distinction between important and unimportant data. The second one is the difficulty to find a meaningful mapping of the measured scalar values to the graphical attributes used for the visualization. These problems are addressed by the special segmentation procedure presented in this paper. The basic idea is to apply graph algorithms to find important structures and to assign multidimensional information to these structures with the help of wavelets. This additional information can be used to generate graphical attributes for rendering. Several aspects emerge from the interaction of both theoretical concepts.

## Introduction

One problem of visualizing medical data by means of volume rendering is, that simple transfer functions are often not sufficient enough to produce meaningful images. This is especially true for MRI data sets, where a measured value may correspond to several types of tissue. In this case the use of transfer functions produces irritating images, as there is little correspondence between the assigned color and the tissue. A first approach to solve this problem has been introduced by Levoy [6] who includes gradient information in the transfer functions. Westermann [10] integrates feature extraction by using the wavelet transformation to evaluate the spatial frequency of the visualized data.

In this paper we present a new method for segmentation and feature extraction for visualization purposes. The main idea is to find and to extract edges from the data set and to compute a feature vector, that may be used for segmentation or for the definition of transfer functions. We developed an algorithm that combines wavelet theory and graph theory, and we applied this to the two dimensional case. We also discuss how these concepts can be generalized to three dimensions.

Edge detection, line segmentation and scale space filtering especially with wavelets became popular and powerful techniques in image segmentation and feature extraction. The basic idea of scale space filtering was first described by Witkin [11]. A filter bank is applied to a given image, which extracts features at different levels of detail. This level of detail aspect was used by Bijaoui [2] to identify different astronomical structures. The filter coefficients for a given point in the image may be directly used as a feature vector as it was proposed by Leite and Hacock [5].

A filter technique, that is capable of scale space filtering, is the wavelet transformation [2, 5]. Many important results about wavelets and feature extraction have been published by Mallat et al. [7, 8, 9]. Berkner et al. [1] analyze the local maxima of the wavelet transformation and the evolution of the wavelet coefficients across different scales to obtain analytical properties of the underlying function which can be used for image segmentation in the medical context.

It can be shown, that the continuous wavelet transformation for a single scale is equivalent to the edge detection method of Canny [3]. Thus, a connection between wavelets and powerful edge segmentation techniques can be established. Several aspects emerge from the interaction of these theories. The Canny operator itself can only detect the maxima for each of the different scales. The wavelet theory provides a framework for obtaining further information, that can be derived from the interaction of the different scales. A commonly used edge processing step is the grouping of pixel maxima into lines for example using graph-theoretical methods as described by Zahn [12]. A different method for detecting strings is the snake method, which requires an initial segmentation of pixels the to drive the external forces. This differs from our approach, where the segmentation is done on the lines themselves. One snake is just capable of finding one closed structure. This differs from our approach, where multiple and also open structures may be segmented.

We present an algorithm, that is capable of identifying lines and of generating a feature vector for every line, that contains information about **(1)** the Euclidean length, **(2)** the Hölder exponent, which is a measure of smoothness, **(3)**

(a) Detected maxima (b) Formed lines (c) Corresponding lines

Figure 1: Stages of the segmentation process

the coarsest scale on which the line has a representation, **(4)** a strength value, that includes gradient information and **(5)** an unsharpness coefficient. In contrast to the approach followed by Hacock [5] the resulting vector does not vary in dimension with the scales involved but the more scales are used the more exact the resulting values will be. A major contribution of this paper is a new algorithm based on wavelets and graphs which generates an appropriate inter-scale interconnection of the extracted lines.

In the following section we describe the overall algorithm. Afterwards, we explain the newly developed details and we finish with some examples. We give analytical examples to validate that the feature vector is computed correctly and a medical example to show the potential of a classification algorithm based on the generated values.

## 1 Overall Algorithm

Several steps have to be performed in order to detect the line structures in the data and to generate the feature vector. First, the local maxima of the wavelet transform have to be computed for every scale. These maxima represent the isolated points shown in Figure 1(a). The coefficients for these maxima are used later on for the calculation of the feature vector. Second, the local maxima of each scale are interconnected into lines using graph theoretical aspects (Figure 1(b)). The interconnection ensures stability of the segmentation process. As lines on different scales may correspond to the same feature in the image, the interdepencies of the lines across different scales have to be established. In Figure 1(c) all lines, that have a correspondence at the second scale are drawn black, and the others are drawn grey. Finally, the feature vector for a line on the first scale can be computed using the average wavelet coefficients of this line at the other scales. Each processing step will be described in more detail in the next sections.

## 2 Construction of Local Maxima

In this section we describe how to find some pixels as atomic structures, which correspond to the local maxima of a continuous wavelet transformation. The wavelet transformation uses two wavelets which are obtained by differentiating the Gauss function in both $x-$ and $y-$ directions. This actually corresponds to using the Canny-Operator for different scale factors.

The multidimensional information which constitutes the feature vector is based on analytical aspects of the underlying function, such as Hölder continuity, gradient absolute value, etc. The wavelet theory provides a framework for analyzing these quantities. The one dimensional wavelet transformation of a function $g \in \mathbf{L^2}(\mathbf{R})$ for a wavelet $\psi$ is defined using the convolution operator

$$(L_\psi g)(a,b) = \frac{1}{a} \int_{-\infty}^{+\infty} g(t) \psi \left( \frac{t-b}{a} \right) \, dt \, , \tag{1}$$

where $b$ is a translation parameter and $a$ a dilatation parameter. For two dimensions the continuous wavelet transformation may be defined using two wavelets $\psi^1$ and $\psi^2$, which are in our case the partial derivatives of the Gaussian function:

$$L_{\psi^1} f(a, x, y) = (f * \psi_a^1)(x, y) \quad (2)$$
$$L_{\psi^2} f(a, x, y) = (f * \psi_a^2)(x, y) \quad (3)$$

Using the partial derivatives of the Gaussian function has the two advantages, that it is infinite continuously differentiable and that it has only one vanishing moment. This guarantees the smoothness of the filtered function on the one hand. On the other hand only singularities with a Hölder exponent smaller than one will be detected, which is a standard requirement for image processing. Furthermore, we are only interested in finding discontinuities of the underlying function. The Hölder exponent is defined as follows: A function $g$ is Hölder continuous $\alpha$ over an open finite interval $\Omega$ if and only if

$$\exists A : \forall x, x_0 \in \Omega : |g(x) - g(x_0)| \leq A|x - x_0|^\alpha . \quad (4)$$

The Hölder exponent describes the continuity qualities of the function. It provides a more differentiated way to express continuity than the standard $C^n$ continuity expression. As edges are singularities of the image, they can be characterized by this exponent. The following theorem describes the relation of the Hölder exponent and the wavelet coefficients.

> The function $g \in \mathbf{L^2}(\mathbf{R^2})$ is uniformly Hölder continuous $\alpha$ on a finite open set $\Omega$ if and only if
>
> $$\exists A : \forall (b \in \Omega) : \forall a : |L_\psi g(a, b)| \leq A a^\alpha \quad (5)$$
>
> holds, where $L_\psi(a, b)$ means the wavelet transformation for the wavelet $\psi$ for translation $b$ and dilatation $a$ (see [7, 8, 9]).

In order to use the results of this theorem one first has to determine the domain, where the Hölder exponent has to be evaluated. Furthermore, one has to find the wavelet coefficients which make (5) as tight as possible.

We are interested in regions around the edges or lines, which are given by local wavelet transform maxima. Because the Gaussian filter tends to disturb and to blur the structures in the data, when the variance becomes large, we will consider such structures which can already be seen for a dilatation parameter $a = 1$. Since one edge has different representations in terms of maxima lines for different dilatation parameters, we consider the problem of building lines from the wavelet transform local maxima in the next section.

## 3 Construction of the lines

In order to construct these lines from the isolated pixels graph theoretical methods are used. An important aspect of the algorithm presented is, that the criteria for operating on the graph to obtain structures which are called lines are motivated by the Gestalt psychology.

Initially, a fully meshed graph is constructed. This graph is divided into a minimal spanning tree. In this work a simpler method has been developed, that performs the construction of the tree from the originally unconnected nodes in one step. This is done using an advancing front technique. Three kinds of nodes are distinguished: nodes that are already *fixed*, nodes that still have not been processed or are *untouched* and nodes that have been processed or *touched*, but whose father can still change. The basic idea of the algorithm is to change one node from *touched* to *fixed* at every iteration. For each one of these nodes the closest k neighbors that are not fixed are analyzed. If their status is *untouched*, they change to *touched* and their father will become *fixed*. If their status is already *touched*, then the length of the root node is compared with the distance of the analyzed *fixed* node. If this distance is shorter, the root of the *touched* node will be changed to the analyzed *fixed* node. This is procedure illustrated in Figure 2.

This tree is separated into several subtrees using the statistical Z-test for the length of each edge and the difference of the wavelet coefficients of the bordering maxima. The processing of the edges works recursively from the root to the trees. If any of the specified values of the edge differs significantly from the mean of the Z-Test of the other edges that lie within a specified hops distance, the tree is truncated into two clusters. The accumulation of the edge values is again done using a recursive mechanism, that searches forward in the direction of the leaves and backwards in the direction of the root.

The generated clusters are separated into lines afterwards. This is done using a gradient criterion and a length criterion for the lines. Every junction is considered. All lines that are closer to the gradient direction than a given angle are eliminated. If the junction still exists after the elimination, then all lines are separated from the junction that does not belong to the longest possible line, that passes through it. These techniques are described in Zahn [12]. The result of this phase is a set of lines for every scale

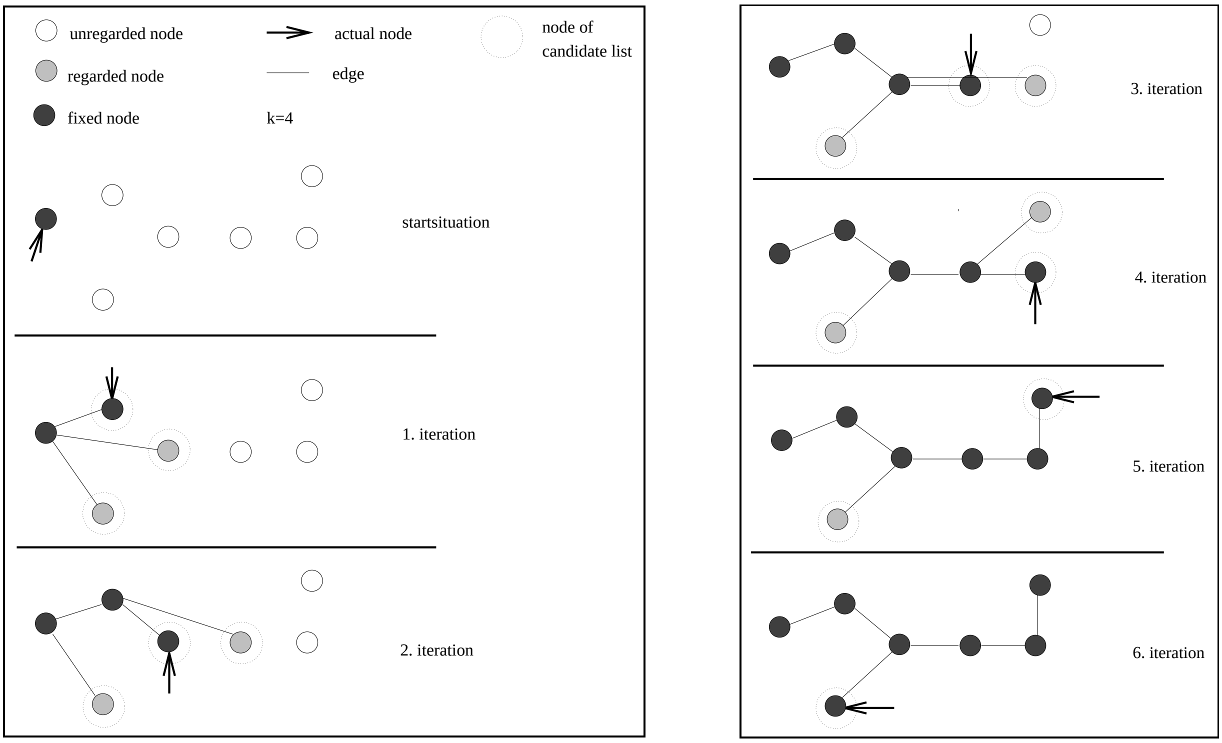


Figure 2: Construction of the minimal spanning tree

## 4 Inter-scale Interconnection

For the evaluation of equation (5) all the corresponding wavelet coefficients for each scaling factor are needed. This means that an interconnection of the lines which belong to the same edge has to be established for different dilatation parameters.

Experimental results have shown, that a simple interconnection between lines is not sufficient, because of the perturbations introduced by the convolution with the Gaussian filter. Depending on the dilatation parameters, lines may be grouped forming completely different structures at different scales. This problem has been solved by means of a carefull regrouping of the lines. The interconnection of the lines between neighboring scales is interleaved with a splitting of the lines at each scale to avoid meaningless interconnections.

For this purpose an initial point to point interconnection, based on the Euclidean distance, is computed. Every node at the scale $n+1$ is connected to its nearest node at the scale $n$. If two nodes at the scale $n+1$ are connected to the same node at the scale $n$, only the shortest link will be kept. This corresponds to a kind of discrete Hausdorff distance.

In a second step a region growing is performed on the lines. The partner lines of the connected points are considered as a homogeneity criterion. The best pairs of already fused segments are fused again. The process stops, when all of them have reached a minimum size and if no further fusion operation can be carried out without corrupting a minimum homogeneity. The resulting points are then fused to segments, that are parts of the lines. New lines that are interconnected across different dilatation parameters are grouped from these segments.

## 5 Computation of the feature vector

When the interconnections have been completed, five characteristic values for each discovered edge can be computed:

- the Euclidean length of the edge,
- the Hölder exponent ($\alpha$),
- the variance where the edge has its last representation,
- the strength, whixh is the factor $A$ in the equation,

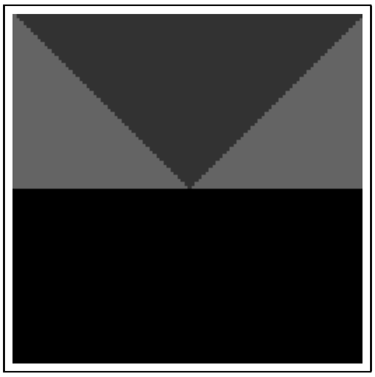

(a) Original image for line detection

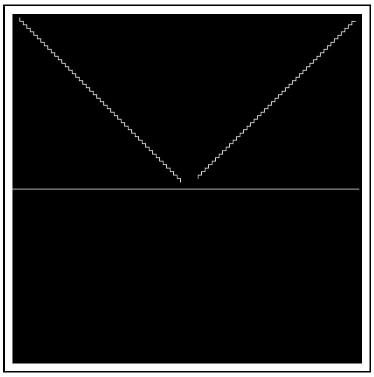

(b) Segmented line

Figure 3: Analytical test data for image segmentation

- and an unsharpness value ($\sigma$), that may be extracted if further assumptions to equation (5) are made (see [8]).

The three characteristic quantities unsharpness, strength and the Hölder exponent are orthogonal quantities. If we assume that the image being considered is the result of a convolution of an unknown image with a convolution kernel of the variance $\sigma$ and if we insert this assumption into equation (5) we get:

$$ln(L_\psi g(a,\vec{b})) \leq ln(A) + ln(a) + \frac{1}{2}(\alpha - 1)ln(a^2 + \sigma^2) \tag{6}$$

This equation contains all the relevant entities which can be derived, if enough wavelet values for different scales are known. Most of the features are computed by means of a least squares approximation to make the resulting inequality as tight as possible. For stability reasons, the mean values and not the maxima of the wavelet coefficients for each dilatation parameter are used. This approach is justified by the fact that there should not be too rapid changes in wavelet coefficients along lines due to the pruning criterion in the graph processing section.

Experiments with a Gauss-Newton approximation have been made, but the approximated function turned out to be too unstable. The gradient descent method has been used instead as suggested in [8].

## 6 Results

In order to illustrate the correctness and the potential of the presented algorithm, two examples are discussed in this section. First we will evaluate the correctness of the discovered values by means of test images. Figure 3(a) is constructed using grey values of 50, 75 and 100. The horizontal line has an Hölder exponent of 0, a strength of 39,89 and an unsharpness of 0. The algorithm discovers the lines shown in Figure 3(b) and computes the following feature values for five evaluated scales: Hölder exponent -0.02, strength 36.71 and unsharpness 0. For seven evaluated scales the results are in even better correspondence: Hölder exponent 0.04, strength 37.4 and unsharpness 0.

As an example for segmentation we have chosen a slice of a MRI-head. Our aim was to segment the skin surface, the surface of the brain and of the ventriculars. We show the limits for the features and the segmentation results for two different MRI slices of two different heads. The skin surfaces in Figures 5(a) and 5(b) have been extracted with the following constraints to the feature vector: length $>$ 0.3, scale $>$ 4, strength $>$ 30. The brain surfaces in Figures 5(c) and 5(d) are found with length $>$ 0.5, 2 $<$ scale $<$ 3 and the ventriculars in Figures 5(e) and 5(f) have been extracted using: 0.01 $<$ length $<$ 0.6, scale $>$ 3, 10 $<$ strength $<$ 36, -1$<$ Hölder exponent $<$ 0, 0.5 $<$ unsharpness $<$ 2.5

Based on our encouraging 2D segmentation results we started extending these techniques to three dimensional applications. Here again, the wavelet transform maxima are used as a starting point for the segmentation process. In three dimensions the graphs can not be used directly, since the result of this technique are lines and not surfaces. In this case, the vertices are interconnected using a Delaunay tetrahedrization. The Delaunay tetrahedrization guarantees, that no other vertices are positioned within the circumsphere of a tetrahedron, than the vertices belonging to the tetrahedron.

The extracted surfaces are surfaces of groups of tetrahedra. The final grouping of lines in the two dimensional case was done using a kind of region growing as described in section 4. In the three dimensional case the tetrahedra

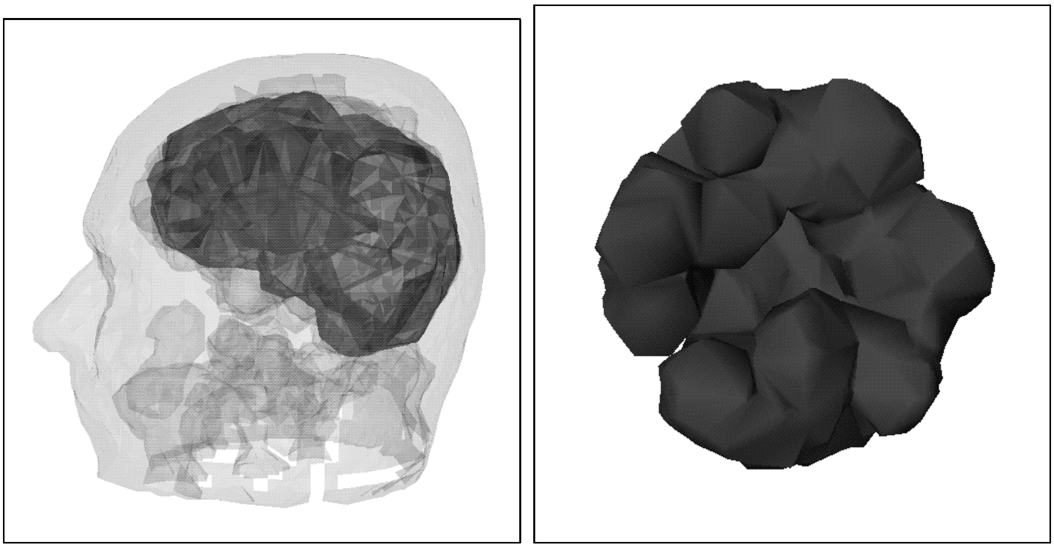

(a) Semi transparent rendering of head and brain surface (b) The ventricular system seen from below

Figure 4: Segmentation of a MRI volume

are also grouped using a region growing technique, where the radius of the circumsphere of a tetrahedron serves as a homogeneity criterion. This is a variation of the $\alpha$-shape concept presented by Edelsbrunner [4]. In this case tetrahedra formations are build of tetrahedra, that have a circumsphere radius below a certain limit.

As a feature vector, the surface to volume ratio, the volume size and the average circumsphere radius is computed. The segmentation result of a MRI head with the brain surface is shown in Figure 4.

This presented technique may also be used for labeling voxels for direct volume rendering or for the integration of the extracted surfaces with direct volume rendering. The brain surface contained in an MRI, can not be visualized with an iso-surface since this would also produce surface elements in other parts of the head. The segmentation procedure, however, offers the potential to separate the brain. Transfer-functions for direct volume rendering can be based on the values of the feature vector instead of the values of the dataset itself since they are a much better characterization of tissue type than the measured absorption values.

## 7 Conclusion

We have shown that the combination of wavelet and graph theory results in a stable segmentation procedure. The results of this process can be used for visualizing medical data sets with quite more meaningful images, than the application of standard mapping methods as transfer functions or isosurfaces derived from the original scalar values. In the future we will extend our first attempts to 3D segmentation by combining $\alpha$-shapes and region growing on the extracted edge information. Furthermore, mechanisms have to be found to determine ranges of characteristic values for interesting medical features.

## References

[1] K. Berkner, C. J. G. Evertsz, and W. Berghorn. Eine lokale charakterisierung von kanten basierend auf skalierungseigenschaften von wavelet-transfomationen. In Carl J.G. Evertsz, editor, *Conference Guide Visualisierung-Dynamik und Komplexität*, September 1995.

[2] A. Bijaoui. Partial reconstruction and astronomical image inventory by the wavelet transform. In *Proceedings ICIAP 1993*, 1993.

[3] J. Canny. A computational approach to edge detection. *IEEE Trans. Patt. Anal. Machine Intell.*, PAMI-8:679–698, 1986.

[4] H. Edelsbrunner and E. P. Mücke. Three dimensional alpha shapes. *ACM Transactions on Graphics*, 13(1):43–72, January 1994.

[5] J.A.F Leite and E. R. Hacock. Statistically combining and refining multi-channel information. In *Proceedings ICIAP 1993*, 1993.

[6] M. Levoy. Display of surface from volume data. *IEEE Computer Graphics and Applications*, 8(3):29–37, 1990.

[7] S. Mallat and W.L. Hwang. Singularity detection and processing with wavelets. Technical report, Courant Institute of Mathematical Sciences New York University, march 1991.

[8] S. Mallat and S. Zhong. Characterization of signals from multiscale edges. *IEEE Transactions on Pattern Analysis and Machine Intelligence*, 14(7):710–732, Juli 1992.

[9] S. Mallat and S. Zhong. Wavelet transform maxima and multiscale edges. In *Wavelets and their Applications*. Boston: Jones and Bartlett Publication, 1992.

[10] R. Westermann. Compression domain rendering of time-resolved volume data. In *IEEE Visualization 1995 Conference Proceedings*, pages 51–58, 1995.

[11] A. Witkin. Scale space filtering. In *Proc. Int. Joint Conf. Artificial Intell.*, 1983.

[12] C. T. Zahn. Graph-theoretical methods for detecting and describing gestalt cluster. *IEEE Transations on Computers*, C-20(1):68–86, 1971.

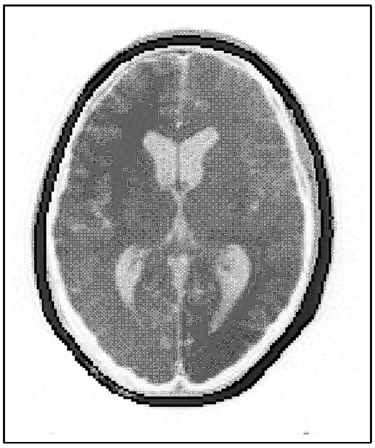

(a) MRI slice 1, skin surface

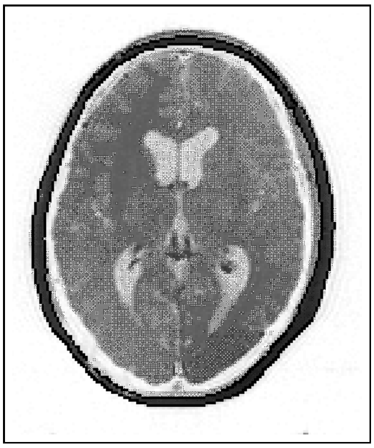

(b) MRI slice 2, skin surface

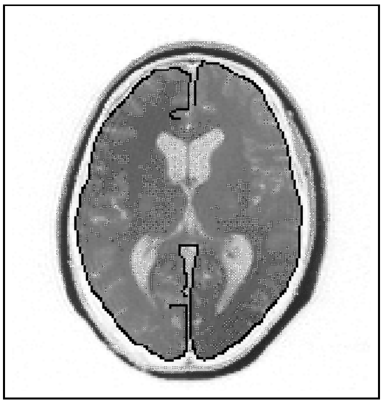

(c) MRI slice 1, brain surface

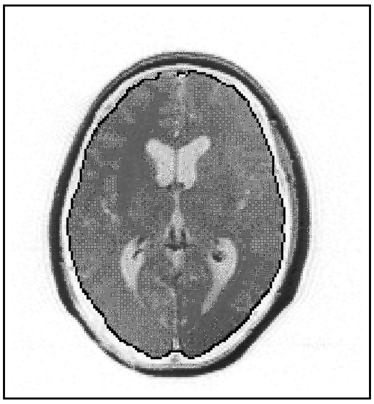

(d) MRI slice 2, brain surface

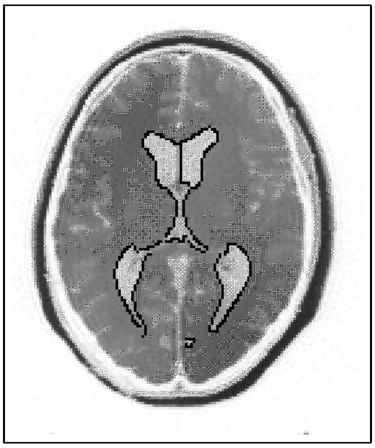

(e) MRI slice 1, ventricle surface

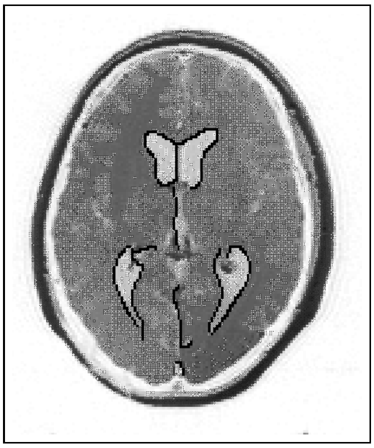

(f) MRI slice 2, ventricle surface

Figure 5: Image Segmentation on two different MRI head slices